

MULTIPARTICLE BREAK-UP OF ^{12}C INDUCED BY NEUTRONS OF 18.2 MeV

B. ANTOLKOVIĆ

Institute Ruđer Bošković, Zagreb

Received 15 March 1976

Abstract: The four-body break-up of the $n + ^{12}\text{C}$ system induced by neutrons of 18.2 MeV has been studied in a kinematically complete experiment. The analysis of the three alpha correlation spectra has shown the predominant contribution of the sequential reaction mechanism, in which the first step proceeds through inelastic neutron scattering, and a very low intensity of the $\alpha + ^9\text{Be}(n, 2\alpha)$ channel. The structure of the momentum distribution of $^8\text{Be}_{gs}$ particles in the ^{12}C nucleus indicates some admixture of the knock-on $^{12}\text{C}(n, n\alpha) \text{Be}_{gs}$ reaction mechanism, but no quantitative results have been extracted so far.

1. Introduction

It has been shown¹⁾ that the $^{12}\text{C}(n, n) 3\alpha$ reaction at a neutron energy of 14.4 MeV can be described completely by a sequential decay process. In this reaction 90% of events proceed via inelastic neutron scattering on ^{12}C , exciting the states above the three-alpha threshold, and the rest of 10% of events decay via the $^{12}\text{C}(n, \alpha)^9\text{Be}(n, 2\alpha)$ channel. On the other hand, it has been found that several neutron-induced multiparticle break-up reactions on light nuclei and at the same neutron energy have a considerable contribution from the quasifree process^{2,3)}. This shows that the role of quasifree scattering should not be neglected even at rather low energy.

The ^{12}C nucleus may be well described by the α - $^8\text{Be}(2\alpha)$ cluster structure, the separation energy of which is 7.38 MeV. Although this value is higher than the separation energies for ^6Li and ^7Li nuclei (1.46 and 2.47 MeV, respectively),

the quasifree process may also be expected in the multiparticle break-up of the ^{12}C nucleus. The question is, however, how much one has to raise the incident neutron energy to reach this situation, since the separation energy of clusters in the target nucleus has a large influence on the knock-on cross section⁴⁾.

There is a limited range of neutron energies (the limit being at 20.4 MeV) where monoenergetic neutron beams can be obtained. At a bombarding energy of 18.2 MeV the energy available in the final channel is increased for $\sim 60\%$ compared with that in the experiment at 14.4 MeV. This increase of energy compensates for the higher separation energy of the alpha cluster in ^{12}C nucleus, so that the total energy delivered to the final channel of the reaction $^{12}\text{C}(n, n\alpha)^8\text{Be}$ becomes approximately the same as that available in the $^7\text{Li}(n, n\alpha)t$ and $^6\text{Li}(n, n\alpha)d$ experiments at 14.4 MeV. The latter reactions, however, show large components of quasifree scattering in the total cross section^{2,3)}.

The presence of $(p, p\alpha)$ and $(\alpha, 2\alpha)$ knock-on reactions on ^{12}C has been confirmed at high bombarding energies⁵⁻⁷⁾. Even at 25 MeV⁸⁾, the experimental data can be fairly well reproduced by the knock-on process, but no conclusions on the reaction mechanism can be drawn when comparing the $(\alpha, 2\alpha)$ experiments at 27 MeV⁹⁾ with those at 38 MeV¹⁰⁾.

The present study of the multiparticle break-up of the ^{12}C nucleus induced by neutrons of 18.2 MeV was performed in order to investigate the reaction mechanism involved in the process, and to get an insight into the contribution of the $(n, n\alpha)$ quasifree scattering to the total yield.

Conditions for a kinematically complete experiment are obtained by measuring the three-alpha products of the $n + ^{12}\text{C} \rightarrow n + 3\alpha$ reaction in the 4π geometry of the nuclear emulsion. These conditions make it possible to deduce the dynamical effects of different processes involved in the reaction. In order to investigate the presence of the sequential-decay mechanism, the data were sorted with respect to the excitation energies of different two- and three-body intermediate states. The momentum distribution of the ^8Be nucleus relative to the remaining alpha particle was extracted to test the contribution of the quasifree-scattering mechanism. A brief description of the method is given, since details are described in earlier papers^{1,2)}.

2. Experimental procedure

Nuclear emulsions are satisfactorily used as a target-detector system for the study of multiparticle break-up reactions if the target nucleus is one of the constituents of the emulsion, or can be loaded in it. They are particularly convenient for the study of the multiparticle break-up of ^{12}C nucleus, because of the high concentration of ^{12}C in nuclear plates (0.207 g/cm^3 or 17.7% of the total number of atoms) and because of the appearance of the $^{12}\text{C}(n, n) 3\alpha$ event as a three-prong star, which differs considerably from a single or two-prong star associated with

other reactions. In the measurement of multiparticle break-up reactions, nuclear emulsions offer several advantages over multidetector systems. These were described in Ref.¹¹⁾

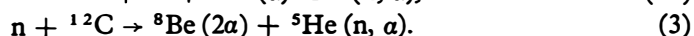
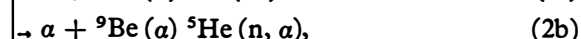
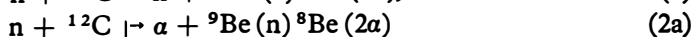
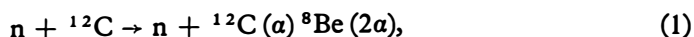
Ilford K2 200 μm plates were exposed to a $1.15 \cdot 10^8 \text{ n/cm}^2$ beam of 18.2 MeV neutrons from the Van de Graaff accelerator. A standard procedure of measuring the length, dip and angle in the horizontal plane was applied to define the energy and spatial directions of all the three-prong of the star. Measurement of energies and directions of three particles gives rise to a kinematic overdetermination of the four-body final state. Since the background of other processes that may appear as three-prong stars is negligible, the overdetermination of the final state, which usually serves for background elimination, was used to improve the energy resolution of the experiment. From the energy spectrum of the incoming neutrons, which was calculated by energy and momentum balance relations, only those events which lie inside the interval of $\pm 2 \text{ MeV}$ around the known bombarding energy were accepted for further analysis.

The experimental data obtained by scanning the plates were registered on magnetic tapes forming a »stored experiment« data set. The information on the dynamics of different reaction mechanisms was obtained by exploiting the same data, but using different computer codes to calculate and sort, under the predetermined kinematical conditions, those variables which are interesting for the analysis of the particular reaction mechanism.

3. Results

The analysis of the data was performed under the assumption that two reaction mechanisms, -sequential decay and quasifree scattering - give the main contribution to the total cross section.

Sequential decay. In the four-body decay $n + {}^{12}\text{C} \rightarrow n + 3\alpha$, the sequential decay may proceed via different channels



In processes (1) and (2) the formation of the intermediate nuclei ${}^{12}\text{C}$ and ${}^9\text{Be}$ is followed by the decay of these nuclei via the ${}^8\text{Be}$ and/or ${}^5\text{He}$ intermediate states. Process (3) represents a double final state $\alpha-\alpha$ and $\alpha-n$ interaction. In order to check whether the latter process contributes to the total cross section, the data were analysed and plotted in a E_{He}^* versus E_{Be}^* triangle representation. This procedure simultaneously tests the occurrence of the two-body clusters ${}^8\text{Be}$ and ${}^5\text{He}$,

since their presence, at least the presence of one of them, is inevitable for the reaction mechanism to be of the sequential-decay type (see processes (1) and (2)). Fig. 1 shows the density distribution of the experimental points in the E_{He}^{α} versus E_{Be}^{α} triangle plot, as well as projections of experimental data onto the E_{He}^{α} and E_{Be}^{α} axes. Due to the indiscernability of the three alpha particles, three different pairs

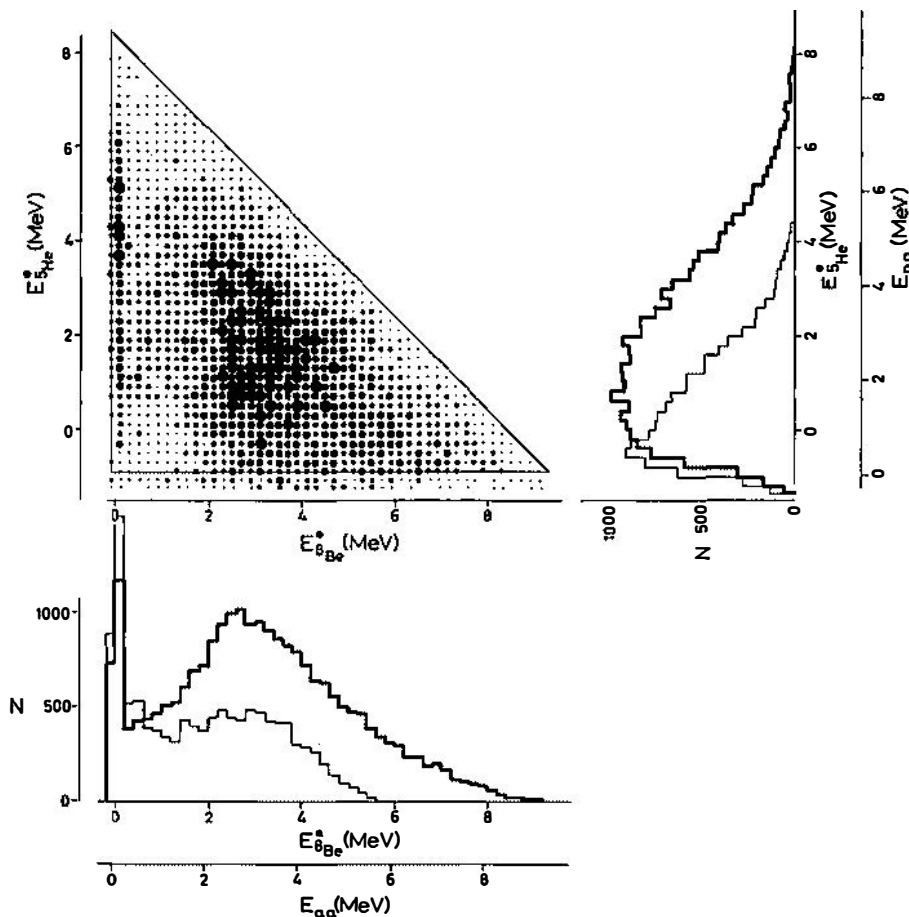


Fig. 1. The density distribution of the experimental points in the E_{He}^{α} versus E_{Be}^{α} triangle plot. The right and lower diagrams (thick lines) are projections of the data onto the E_{He}^{α} and E_{Be}^{α} (or $E_{\alpha\alpha}$ and $E_{\alpha\alpha}$) axes, respectively. The thin line histograms are the corresponding spectra obtained in the experiment at 14.4 MeV¹⁾.

$a_i - a_j$, $a_k - n$ can be calculated by permuting the indices i, j and k ; hence each event is represented in the diagram by three-data points. Only one third of all the data are thus »true« and these are superimposed onto a continuum formed by two thirds of »spurious events«. This difficulty has to be taken into account in the analysis of the data. The density distribution of the triangle diagram in Fig. 1 shows

an enhancement of data in a narrow band around $E_{8\text{Be}}^* = 0.0$ MeV and in the middle of the diagram. By projecting the data onto the $E_{8\text{Be}}^*$ axis, a distinct peak appears which corresponds to the transition via the 0^+ ground state of ^8Be . The broad structure around $E_{8\text{Be}}^* = 3.0$ MeV corresponds to the superposition of the 2.9 MeV level of 1.4 MeV width to the continuum formed by spurious excitations and possible contributions of other reaction channels. From the kinematical considerations it can be deduced (see also Fig. 4 of Ref. ¹⁾) that in those events in which one α - α combination is associated with $^8\text{Be}_{\text{gs}}$, the »true« values for the ^8Be excitation energies cluster in a narrow peak well separated from the continuum formed by »spurious« values. The $^8\text{Be}_{\text{gs}}$ transition may thus be successfully resolved from the spurious events. For the transition via the $^8\text{Be}_{2,9}$ state, such a distinction could not be made, due to the overlap of these two components.

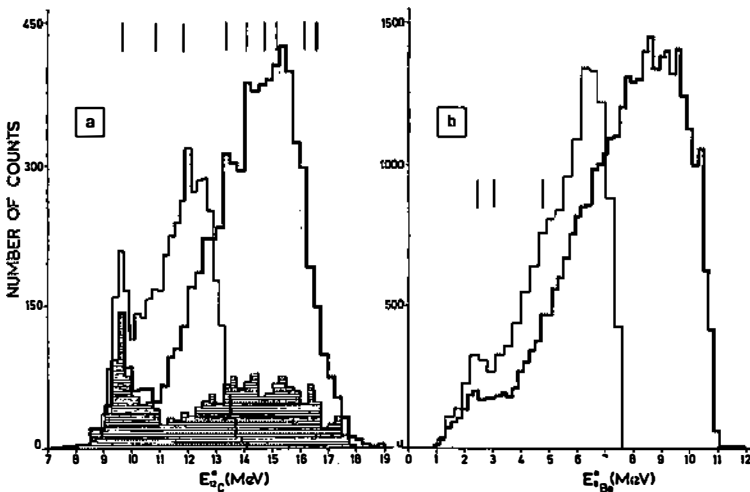


Fig. 2. The spectra of the excitation energies of the: a) ^{12}C , and b) ^9Be intermediate nuclei. The bars indicate the positions of the energy levels of the ^{12}C and ^9Be nuclei, respectively. The shaded histogram in Fig. 2a is the ^{12}C excitation energy spectrum of the events which proceed via the $^8\text{Be}_{\text{gs}}$ intermediate state.

As seen from Fig. 1, there is no visible clustering of data on the $^5\text{He}_{\text{gs}}$ locus of the triangle diagram, nor any evidence for the enhancement of data on the intersection of this locus with the $^8\text{Be}_{\text{gs}}$ locus. This indicates that the contribution of process (3) to the total cross section is insignificant. The corresponding results obtained at 14.4 MeV, represented by the thin line histograms in the projected spectra of Fig. 1, are given for comparison (no normalization was performed, the frequencies given are those obtained in experiments, respectively).

The spectra of the excitation energies of the ^{12}C and ^9Be intermediate-state nuclei, formed in processes (1) and (2), are shown in Fig. 2. Again, the thin line histograms present the corresponding spectra obtained in the experiment

at 14.4 MeV. It should be noted that the E_{Be}^{\dagger} diagram has three times more data points than the E_{C}^{\dagger} diagram, since there are three values of the ${}^9\text{Be}$ excitation energy for each event, while the excitation energies of ${}^{12}\text{C}$ are single-valued. The shaded histogram in Fig. 2a contains only those events for which the ${}^8\text{Be}$ excitation of one pair of alpha particles is $E_{\text{Be}}^{\dagger} = 0.0 \pm 0.1$ MeV; hence it represents the contribution of the sequential decay via the ${}^8\text{Be}_{\text{gs}}$ intermediate state in different regions of ${}^{12}\text{C}$ excitations.

Simultaneous inspection of the E_{C}^{\dagger} and E_{Be}^{\dagger} spectra of Fig. 2 indicates the predominant contribution of the sequential decay by process (1). In the excitation spectrum of ${}^{12}\text{C}$, the strongly excited level at 9.63 MeV is well separated from the rest of the spectrum. There is a sharp cut off of the data below this level; although the phase space distribution will allow the data to be present down to 7.27 MeV (the ${}^{12}\text{C}_{7,65}$ level lies immediately above the 3α threshold and the amount of energy distributed to alpha particles is too small for this level to be registered

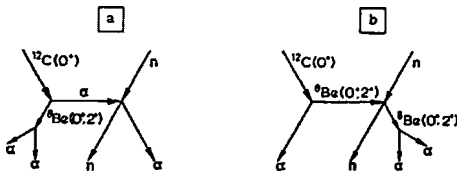


Fig. 3. Graphs of the quasifree scattering process with: a) ${}^8\text{Be}$ particle, and b) alpha particle as a spectator.

in nuclear emulsions). The presence of some higher levels is also noticeable, although these levels could not be resolved due to the angular and energy resolution of the measurement. The continuous shape of the ${}^9\text{Be}$ excitation spectrum (which is equivalent to the E_{α} distribution in the centre of mass of ${}^{13}\text{C}$) is the result of the 3α decay of the ${}^{12}\text{C}$ levels, confirming once more that process (1) is the dominant reaction mode.

A superposition of a certain structure at low ${}^9\text{Be}$ excitations may be attributed to process (2) which proceeds via the 2.43 MeV state of ${}^9\text{Be}$. Its intensity is, however, considerably lower than that at a bombarding energy of 14.4 MeV, and only an estimate of its contribution to the total yield can be made.

Quasielastic scattering. The quasielastic scattering of neutrons may occur on both constituents of the ${}^{12}\text{C}$ cluster structure, the alpha and the ${}^8\text{Be}$ particle. The two processes are represented by graphs a and b in Fig. 3. It can be seen that graph 3a offers more defined experimental conditions since:

- the two components of each graph, corresponding to either the ${}^8\text{Be}_{\text{gs}}$ or ${}^8\text{Be}_{2,9}$ state (the relative angular momentum of the alpha- ${}^8\text{Be}$ motion being $l = 0$ and $l = 2$, respectively) can be separated experimentally in graph 3a, but not in graph 3b;
- the differential cross sections for the n- α scattering are well known, which is not the case for the n- ${}^8\text{Be}$ differential cross sections.

As mentioned in chapter *Sequential decay*, the ${}^8\text{Be}_{\text{gs}}$ excitations can be extracted experimentally free of spurious events, while for the ${}^8\text{Be}_{2,9}$ state the true events are superimposed onto the continuum of the two thirds of spurious events. Because

of all these facts the following analysis will be concentrated only on the $^{12}\text{C}(n, \alpha)^8\text{Be}_{\text{gs}}$ reaction.

The analysis was performed by plotting the ^8Be momentum distribution of those events for which one pair of particles has $E_{\text{Be}}^* = 0.0 \pm 0.1$ MeV. The plane-wave-impulse approximation was applied to extract the momentum distribution $[\Phi(p)]^2$ of ^8Be particles in the ^{12}C nucleus. Each datum point in the momentum distribution of $^8\text{Be}_{\text{gs}}$ was corrected for the corresponding phase-space factor and the differential n - α cross section, interpolated with respect to angle and energy²⁾. The off-energy-shell n - α scattering cross sections were replaced by the free n - α cross sections at the relative energy of the two scattered particles.

Fig. 4 shows the extracted momentum distribution $[\Phi(p)]^2$ of $^8\text{Be}_{\text{gs}}$ particles in the ^{12}C nucleus. The thick line histogram contains all data that proceed via the ground state of ^8Be . Inspection of Fig. 2a shows that part of these data proceed via a sequential decay process (at least those, going via the $^{12}\text{C}_{9,63}$ excited state). To check their influence on the $[\Phi(p)]^2$ distribution a thin line histogram was constructed of data pertaining to the $^{12}\text{C}(n, n)^{12}\text{C}_{9,63}(\alpha)^8\text{Be}_{\text{gs}}(2\alpha)$ channel ($E_{12\text{C}}^* = 9.63 \pm 1.0$ MeV). The lack of data below 110 MeV/c in both distributions is due to the experimental bias for detecting alpha particles of energy less than 0.3 MeV. It can be seen that the thick line histogram has a definite structure, while the thin line histogram exhibits a smooth behaviour within the statistical errors. The same continuous shape distribution would also be expected from other reaction components proceeding via the sequential decay. On the ground of the $l = 0$ α - $^8\text{Be}_{\text{gs}}$ structure of ^{12}C , one expects a momentum distribution peaked at zero momentum. The increasing trend of the experimental distribution towards the low cut-off can be explained as a tail of such a distribution. A maximum which is visible in the spectrum was also obtained in $^{12}\text{C}(\alpha, 2\alpha)^8\text{Be}$ experiments at 27 MeV⁹⁾ and 90 MeV^{**)} and is predicted by the theoretical momentum distribution. The dashed curve in Fig. 4 is the Fourier transform of the wave function of the relative α -Be motion in $^{12}\text{C}^{**)$. The radial wave function of alpha clusters is represented by the harmonic oscillator function and the value of R is 4.5 fm, which reproduces a good theoretical fit to the experimental ^8Be excitation energy spectrum¹²⁾. The structure of the experimental momentum distribution could thus be qualitatively explained as an admixture of the knock on $^{12}\text{C}(n, \alpha)^8\text{Be}_{\text{gs}}$

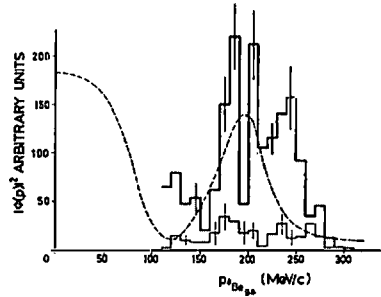


Fig. 4. The momentum distribution $[\Phi(p)]^2$ of the $^8\text{Be}_{\text{gs}}$ in the ^{12}C nucleus (thick line histogram). The thin line histogram presents the momentum distribution of data, which proceed via the $^{12}\text{C}_{9,63}$ intermediate state. The dashed curve is the theoretical momentum distribution^{**)}.

***) C. Jacquot, private communication.

reaction to the sequential decay mechanism. However at an energy of 18.2 MeV it is still not possible to draw definite conclusions on the amount of the contribution of this reaction to the total cross section.

4. Conclusion

The analysis of the three-alpha correlation spectra has shown that the cross section of the four-body break-up of the $n + {}^{12}\text{C}$ system is dominated by the sequential-decay mechanism. Process (1), inelastic neutron scattering on ${}^{12}\text{C}$, and its subsequent decay into three alpha particles gives a predominant contribution to the total cross section. The decay via the ${}^8\text{Be}_{gs}$ in the reaction chain (1) is, however, considerably less favoured than it was in the case of the experiment at 14.4 MeV. The other possible sequential-decay channels receive only a small contribution (less than 5% of the total yield) from process (2), ${}^{12}\text{C}(n, \alpha){}^9\text{Be}_{2,4,3}(n, 2\alpha)$. It is, however, interesting to note that there is no evidence for the enhancement of the data on the intersection of the $E_{8\text{Be}}^* = 0.0$ and $E_{5\text{He}}^* = 0.0$ lines in the triangle diagram of Fig. 1. This would indicate an alpha pick-up ${}^{12}\text{C}(n, {}^5\text{He}){}^8\text{Be}$ process, which pole graph diagram is simpler than that of the two-body knock-on ${}^{12}\text{C}(n, \alpha){}^9\text{Be}$ reaction, present in the $n + {}^{12}\text{C} \rightarrow n + 3\alpha$ decay. Since the contribution of the process (2) is small and no contribution is received from process (3), the rate of the sequential transition through the ${}^5\text{He}$ intermediate state is low, almost negligible. This is, however, common feature to the ${}^{12}\text{C}(n, \alpha){}^9\text{Be}$ and ${}^{12}\text{C}(p, \alpha){}^9\text{B}$ reactions, since the latter¹³⁻¹⁶⁾ also show peaks of ${}^9\text{B}$ states which are of weak intensity (disintegrating via the mass 5 system, $\text{B}(\alpha){}^5\text{Li}(p, \alpha)$), superimposed onto a large continuum resulting from the ${}^{12}\text{C} \rightarrow 3\alpha$ decay.

The analysis of the data in the framework of the PWIA has shown a certain structure of the momentum distribution of ${}^8\text{Be}_{gs}$ in the ${}^{12}\text{C}$ nucleus, that could be attributed to the quasifree-scattering process. However, its intensity is weak and could be only qualitatively established.

Acknowledgement

The author is indebted to Professor M. Bormann for offering the facilities of the Van de Graaff accelerator at Institut für Experimentalphysik, Hamburg and to Dr. M. Scobel for performing the irradiation of the plates.

References:

- 1) B. Antolković, Nucl. Phys. **A237** (1975) 235;
- 2) B. Antolković, Nucl. Phys. **A219** (1974) 332;
- 3) B. Antolković and M. Turk, Proceedings of the Second Intern. Conference on Clustering Phenomena in Nuclei, College Park, Maryland (1975) 307;

- 4) Y. Sakamoto, P. Cüer and F. Takéutchi, Phys. Rev. **C11** (1975) 668;
- 5) T. Yuasa, Phys. Lett. **8** (1964) 318;
- 6) A. N. James and H. G. Pugh, Nucl. Phys. **42** (1963) 44;
- 7) G. Igo, L. F. Hansen and T. J. Gooding, Phys. Rev. **131** (1963) 337;
- 8) V. K. Dolinov, Yu. V. Melikov, A. Tulinov and O. Bormot, Nucl. Phys. **A129** (1969) 577;
- 9) T. Yanabu, S. Yamashita, K. Takimoto and K. Ogino, J. Phys. Soc. Jap. **20** (1965) 1303;
- 10) T. Yanabu, S. Yamashita, K. Hosono, S. Matsuki, T. Tanabe, K. Takimoto, Y. Okuma, K. Ogino, S. Okumura and R. Oshiwari, J. Phys. Soc. Jap. **24** (1968) 667;
- 11) B. Antolković, *Proced. of a Pannel Meeting on the Utilization of Low Energy Accelerators, IAEA-171* (1975) 223;
- 12) C. Jacquot, Y. Sakamoto, M. Jung, C. Baixeras-Aiguabella, L. Girardin and H. Braun, Nucl. Phys. **A148** (1970) 325;
- 13) J. L. Need, Phys. Rev. **99** (1955) 1356;
- 14) S. S. Vasileyev, V. V. Komarov and A. M. Popova, Nucl. Phys. **40** (1963) 443;
- 15) G. D. Symons, Phys. Lett. **10** (1964) 89;
- 16) M. M. Islam and P. B. Treacy, Nucl. Phys. **70** (1965) 236.

VIŠEČESTIČNI RASPAD JEZGRE ^{12}C PRI UPADNOJ ENERGIJI NEUTRONA OD 18.2 MeV

B. ANTOLKOVIĆ

Institut Ruđer Bošković, Zagreb

Sadržaj

Mjeren je četveročestični raspad sistema $n + ^{12}\text{C}$ u kinematsko kompletnom eksperimentu pri upadnoj energiji neutrona od 18.2 MeV. Analiza korelacionih spektara 3 alfa čestica pokazuje da najveći doprinos procesu sukcesivnog raspada daje reakcija koja se odvija putem inelastičnog raspršenja neutrona na jezgri ^{12}C . Sukcesivni raspad preko $\alpha + ^9\text{Be}(n, 2\alpha)$ kanala vrlo je malog intenziteta.

Struktura raspodjele impulsa čestica $^8\text{Be}_{gs}$ u jezgri ^{12}C ukazuje na postojanje kvazislobodnog procesa $^{12}\text{C}(n, n\alpha)^8\text{Be}$, no njegov je doprinos kod 18.2 MeV još uvijek premalen da bi se mogli izvući kvantitativni rezultati.